SIAM J. APPL. MATH.
Vol. 67, No. 3, pp. 605–618

NONLINEAR ANALYSIS IN THE AW–RASCLE ANTICIPATION MODEL OF TRAFFIC FLOW*

ZHONG-HUI OU†, SHI-QIANG DAI†, PENG ZHANG†, AND LI-YUN DONG†

Abstract. In this paper, the Aw–Rascle anticipation (ARA) model is discussed from the perspective of the capability to reproduce nonlinear traffic flow behaviors observed in real traffic. For this purpose, a nonlinear traffic flow stability criterion is derived by using a wavefront expansion technique. The result of the nonlinear stability analysis can be used not only to judge the stability evolution of an initial traffic state but also to determine the pressure term in the ARA model. The KdV equation is derived from the ARA model added by the viscous term with the use of the reduction perturbation method. The soliton solution can be analytically obtained from the perturbed KdV equation only near the neutral stability line. Weighted essentially nonoscillatory schemes are employed to simulate the KdV soliton. The numerical results confirm the analytical KdV soliton solution.

Key words. traffic flow, soliton, WENO

AMS subject classifications. 35L65, 41A58

DOI. 10.1137/060656863

1. Introduction.

A macroscopic model of vehicular traffic started with the first-order fluid approximation of traffic flow dynamics proposed by Lighthill, Whitham [1], and Richards [2] independently, i.e., the Lighthill–Whitham–Richards (LWR) model [3], which assumes the conservation of the number of vehicles and the equilibrium relation between flow and density. However, besides the continuity equation, one needs an extra dynamic velocity equation in order to describe the emergent traffic jams and stop-and-go traffic. This kind of two-equation model includes the Payne–Whitham (PW) model [4, 5, 1], the Kühne model [6, 7], the Kerner–Konhäuser (KK) model [8, 9], the Lee–Lee–Kim (LLK) model [10, 11], the gas-kinetic-based (GKT) model [12, 13, 14, 15], etc. But Daganzo pointed out that one characteristic velocity greater than the macroscopic fluid velocity in the two-equation models would lead to nonphysical effects [16]. Aw and Rascle replaced the space derivative of the "pressure" with a convective derivative in PW-type models to resolve the theoretical inconsistencies and then constructed the Aw–Rascle anticipation (ARA) model [17, 18, 19]. They discussed the solution to the Riemann problem and the admissibility of the elementary waves by the hyperbolic conservation laws in detail. Moreover, the ARA model is the typical form of the anisotropic traffic flow model, which can be reduced to other models from different viewpoints [20, 21].

A traffic flow model usually needs stability analysis and numerical simulation in the stable and unstable density regions in order to investigate the evolution of a traffic initial state [8, 12, 22, 20, 23, 24, 25, 26]. Since in the linear stability analysis higher-order terms are neglected, we propose a nonlinear stability analysis by utilizing

*Received by the editors April 10, 2006; accepted for publication (in revised form) October 19, 2006; published electronically February 23, 2007. This work was financially supported by the National Basic Research Program of China (the 973 Program) under grant 2006CB705500, the National Natural Science Foundation of China under grant 10532060, the Shanghai Postdoctoral Scientific Program, and the Shanghai Leading Academic Discipline Project (Y0103).

http://www.siam.org/journals/siap/67-3/65686.html

†Shanghai Institute of Applied Mathematics and Mechanics, Shanghai University, Shanghai 200072, People's Republic of China (ouzhonghui@vip.sina.com, sqdai@shu.edu.cn, pzhang@mail.shu.edu.cn, lydong@mail.shu.edu.on).

a wavefront expansion technique under large traffic disturbances. Moreover, some typical nonlinear waves such as the KdV soliton, triangular shock, and kink have been found through investigating the car-following models with the reduction perturbation method [27, 28, 29], but only Kurtze and Hong [30] and Berg and Woods [31] did similar work in the continuum model. The reduction perturbation method is more difficult to conduct in the continuum model than in the car-following model because the former has a much more complicated form than the latter. Therefore it is valuable for the anisotropic ARA model to make the nonlinear stability and wave analysis in traffic flow.

This paper is arranged as follows. We take the nonlinear stability analysis on the ARA model, and one stability criterion is used to determine the pressure term in section 2. The KdV equation is derived from the ARA model with the viscous term in section 3. Weighted essentially nonoscillatory schemes (WENO) schemes are used to simulate the KdV soliton in section 4. Concluding remarks are presented in section 5.

2. Nonlinear stability analysis. The ARA model is

$$\partial_t \rho + \partial_x(\rho v) = 0, \tag{1}$$

$$\partial_t(v + p(\rho)) + v\partial_x(v + p(\rho)) = \tau^{-1}(V(\rho) - v), \tag{2}$$

where $\rho(x,t)$ is the density at point x and time t, $v(x,t)$ is the velocity, τ is the relaxation time, $V(\rho)$ is the equilibrium function, $p(\rho) = \rho^\gamma$ is the pressure (the anticipation factor is more accurate), and γ is a positive constant which needs to be determined later [17]. The ARA model under conservative form is

$$\partial_t Y + \partial_x(f(Y)) = g(Y), \tag{3}$$

where the conservative vectors $Y = (\rho, y) = (\rho, \rho(v+p(\rho)))$, $f(Y) = (\rho v, \rho v(v+p(\rho)))$, and $g(Y) = \big(0, \tau^{-1}\rho(V(\rho) - v)\big)$.

The eigenvalues of (1) and (2) are

$$\lambda_1 = v - \rho p'(\rho) \le \lambda_2 = v. \tag{4}$$

Formula (4) shows that all the waves propagate at a speed at most equal to the velocity v of the corresponding state. Daganzo has pointed out that continuum models (especially the hydrodynamic models) with one characteristic speed greater than the macroscopic fluid velocity encounter difficulties showing nonphysical effects in certain situations [16]. But the ARA model avoids these difficulties.

When the traffic jam happens, the density of the traffic jam is much higher than that of the neighboring section, so most traffic jams belong to large disturbances. When the disturbance is fairly large, the linearization method may produce incorrect results because of neglecting higher-order terms as pointed out by Whitham [1], which is the primary cause we propose a nonlinear stability analysis for traffic flow [1, 22, 23, 24]. If a disturbance starts at position x_0 in the homogeneous state of traffic flow, the wavefront is the propagation curve of the disturbance along the homogeneous traffic flow [1, 22, 23, 24]. The magnitude of the initial disturbance will not increase during its propagation if the traffic system is stable in propagation; otherwise, a disturbed density or velocity wave may increase in magnitude as it propagates upstream and ultimately form a shock wave or traffic jam on the highway. If the form of the initial density disturbance is given, the initial velocity disturbance can be determined by the equilibrium function. Furthermore, the profiles of density and velocity disturbances

are symmetrical to some degree along the x-axis in the simulation with the continuum model (e.g., monotone increase vs. monotone decrease, concavity vs. convexity, etc.) [8, 9, 15], which is still considered valid in the ARA model, and this fact will also be demonstrated by the following numerical simulation of the KdV soliton. Therefore, when we merely demand some mathematical assumptions for the density, they are automatically needed for the velocity, and most results are presented for either the density or the velocity. Assume that a disturbance initiates from the equilibrium state (ρ_0, v_0), the solutions of (1) and (2), in the homogeneous traffic flow. If the mth derivatives of ρ around the wavefront WF are the first ones to be discontinuous, the expanded Taylor series from ρ_0 starts with the term in the mth power of a small parameter, which is equally assumed for v_0. Without losing generality, we might as well assume that the first derivative of the density around the wavefront WF is discontinuous.

It is convenient to expand the solution of the system around the wavefront WF in powers of

$$\xi = x - X(t), \tag{5}$$

where $X(t)$ is the location of the wavefront WF at time t. Since the wavefront is the boundary of the disturbance in the homogeneous state, the characteristic method is still feasible in the near neighborhood of the wavefront WF. Therefore the wavefront has the characteristic velocity $v_{c1,2}$ in the equilibrium states, i.e.,

$$\dot{X}(t) = v_{c1,2}(\rho_0, v_0) = v_0 - \lambda_{1,2}. \tag{6}$$

Using (5), we can expand the flow variables ρ, v, their partial derivatives, $V(\rho)$ and $p_\rho(\rho)$, etc., in the power series of ξ as

$$\rho(x,t) = \rho_0 + \xi\rho_1(t) + \frac{1}{2}\xi^2\rho_2(t) + \cdots, \tag{7}$$

$$v(x,t) = v_0 + \xi v_1(t) + \frac{1}{2}\xi^2 v_2(t) + \cdots, \tag{8}$$

where

$$\rho_i(t) = \frac{\partial^i \rho}{\partial x^i}\bigg|_{(X(t)^-,t)}, \quad v_i(t) = \frac{\partial^i v}{\partial x^i}\bigg|_{(X(t)^-,t)}, \quad i = 1,2,3,\ldots,$$

$$\rho_t = -\dot{X}(t)\rho_1(t) + \xi\dot{\rho}_1(t) + \xi\left[-\dot{X}(t)\right]\rho_2(t) + \frac{1}{2}\xi^2\dot{\rho}_2(t) + \cdots, \tag{9}$$

$$\rho_x = \rho_1(t) + \xi\rho_2(t) + \frac{1}{2}\xi^2\rho_3(t) + \cdots, \tag{10}$$

$$v_t = -\dot{X}(t)v_1(t) + \xi\dot{v}_1(t) + \xi\left[-\dot{X}(t)\right]v_2(t) + \frac{1}{2}\xi^2\dot{v}_2(t) + \cdots, \tag{11}$$

$$v_x = v_1(t) + \xi v_2(t) + \frac{1}{2}\xi^2 v_3(t) + \cdots. \tag{12}$$

$$V(\rho) = V^0 + \xi V_\rho^0\rho_1(t) + \cdots, \tag{13}$$

where

$$V^0 = V(\rho_0) \quad \text{and} \quad V_\rho^0 = \frac{\partial V}{\partial \rho}\bigg|_{(\rho_0,v_0)}.$$

$$p_\rho(\rho) = p_\rho^0 + \xi p_{\rho\rho}^0\rho_1(t) + \cdots. \tag{14}$$

Substituting (7)–(14) into (1) and (2), for the coefficients of the first two terms ξ^0 and ξ^1, we obtain

$$u_0\rho_1 + \rho_0 v_1 = 0, \tag{15}$$

$$\dot{\rho}_1 + 2\rho_1 v_1 + u_0\rho_2 + \rho_0 v_2 = 0, \tag{16}$$

$$v_1 + p_\rho^0 \rho_1 = 0, \tag{17}$$

$$u_0 v_2 + u_0 p_\rho^0 \rho_2 + \dot{v}_1 + v_1^2 + p_\rho^0 \dot{\rho}_1 + u_0 p_{\rho\rho}^0 {\rho_1}^2 + v_1 p_\rho^0 \rho_1 + \tau^{-1}\left(v_1 - V_\rho^0 \rho_1\right) = 0, \tag{18}$$

where $u_0 = \lambda_{1,2}$.

Substituting (15) into (17) yields

$$u_0 - \rho_0 p_\rho^0 = 0, \tag{19}$$

which shows that the coefficients of terms ρ_2 and v_2 are linearly dependent and can be eliminated from (16) and (18). Inserting $\rho_1 = -\rho_0 v_1/u_0$ obtained from (15) into (16) and (18) leads to the Bernoulli equation

$$\dot{v}_1 + \alpha v_1 + \beta v_1^2 = 0, \tag{20}$$

where

$$\alpha = \tau^{-1}\left(1 + \frac{V_\rho^0}{p_\rho^0}\right) \quad \text{and} \quad \beta = 2 + \frac{\rho_0 p_{\rho\rho}^0}{p_\rho^0} = \gamma + 1.$$

$\beta > 0$, if $p(\rho) = \rho^\gamma, \gamma > 0$.

If $\alpha = 0$, the solution of (20) is

$$v_1(t) = \frac{v_1(0)}{\beta v_1(0)t + 1}, \tag{21}$$

whose monotonicity is determined by

$$v_1'(t) = -\frac{\beta v_1^2(0)}{(\beta v_1(0)t + 1)^2}. \tag{22}$$

This situation is depicted in Figure 1.

If $\alpha \neq 0$, (20) has two constant solutions,

$$v_1^1(t) \equiv 0 \quad \text{and} \quad v_1^1(t) \equiv -\frac{\alpha}{\beta}, \tag{23}$$

and a general solution,

$$v_1(t) = \frac{\alpha}{\beta}\frac{e^{-\alpha t}}{\left[1 + \frac{\alpha}{\beta v_1(0)}\right] - e^{-\alpha t}}, \tag{24}$$

whose monotonicity is determined by

$$v_1'(t) = -\frac{\alpha^2}{\beta}\frac{\left[1 + \frac{\alpha}{\beta v_1(0)}\right] e^{-\alpha t}}{\left\{\left[1 + \frac{\alpha}{\beta v_1(0)}\right] - e^{-\alpha t}\right\}^2}. \tag{25}$$

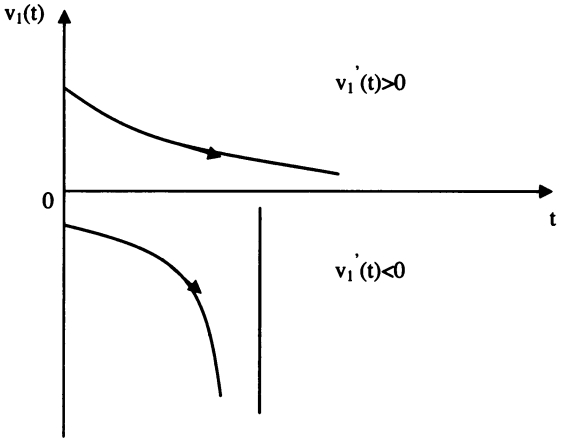

FIG. 1. $\alpha = 0$, $\beta > 0$. $v_1(t)$ *is the partial derivative of velocity.*

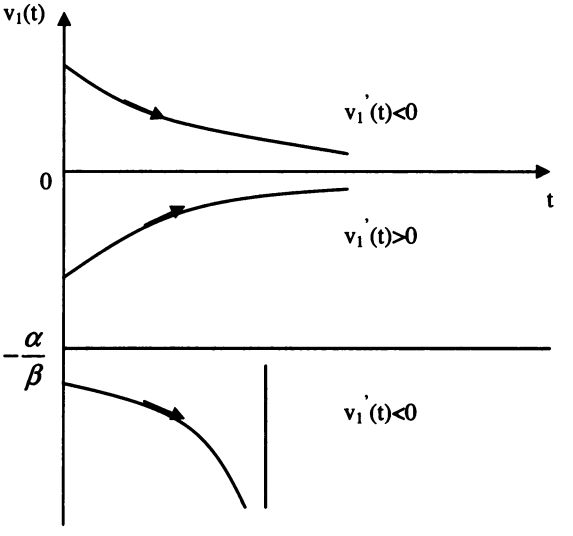

FIG. 2. $\alpha > 0$, $\beta > 0$.

This situation is depicted in Figures 2 and 3. Therefore we can judge the trend of $v_1(t)$ in the light of the parameter α and the initial equilibrium state according to Table 1. Without loss of generality, if the density disturbance is upward, the velocity perturbation is downward, i.e., $v_1(0) < 0$. If $v_1(0) \in [-\alpha/\beta, 0]$, $\alpha > 0$, i.e.,

$$V_\rho > -p_\rho. \tag{26}$$

The system is stable for traffic flow disturbances; otherwise, the system is unstable under $v_1(0) < 0$ and $\alpha < 0$, which is identical to the linear stability criterion. The linear stability result is usually only one condition obtained from the nonlinear analysis [22, 23]. Furthermore, the nonlinear stability results predict the ultimate trend of the slope of disturbance around the wavefront WF, i.e., converging to zero or diverging to negative infinity, which cannot be obtained from the linear stability analysis.

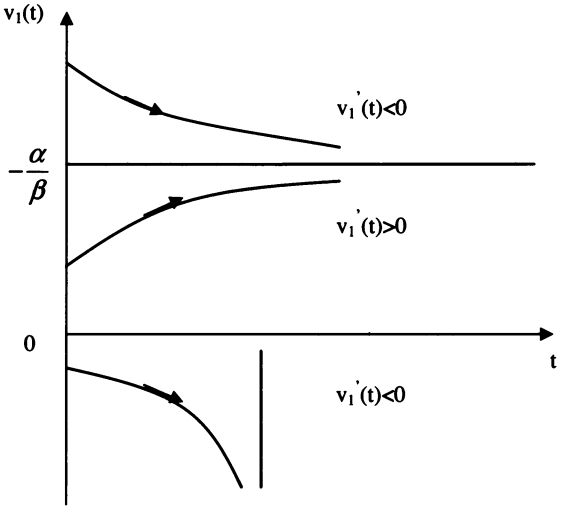

FIG. 3. $\alpha < 0$, $\beta > 0$.

TABLE 1
Stability conditions of (20).

α	Stable region	Unstable region
$\alpha > 0$	$v_1(0) \in (-\frac{\alpha}{\beta}, +\infty), v_1(t) \to 0$	$v_1(0) \in (-\infty, -\frac{\alpha}{\beta}), v_1(t) \to -\infty$
$\alpha = 0$	$v_1(0) \in (0, +\infty), v_1(t) \to 0$	$v_1(0) \in (-\infty, 0), v_1(t) \to -\infty$
$\alpha < 0$	$v_1(0) \in [0, +\infty), v_1(t) \to -\frac{\alpha}{\beta}$	$v_1(0) \in (-\infty, 0), v_1(t) \to -\infty$

Hydrodynamic models with equilibrium functions have been used to obtain reliable results which can reflect the real traffic [8, 9, 12, 15]. Although the ARA model doesn't belong to the hydrodynamic model, they are both higher-order continuum models, and we substitute the abstract form in the ARA model with the equilibrium functions given in previous hydrodynamic models, which are related to the time-independent and homogeneous traffic flow and are fitted by empirical data [4, 5, 8]. Some equilibrium functions established recently actually approach each other in the fundamental diagram [23, 24], and we choose a representative one, i.e., the KK equilibrium function first used in the KK model [8, 9], to displace the abstract form in the ARA model:

$$V(\rho) = V_f \left[\left(1 + \exp\left\{ \frac{\frac{\rho}{\rho_j} - 0.25}{0.06} \right\} \right)^{-1} - 3.72 \times 10^{-6} \right], \tag{27}$$

where V_f is the free flow velocity and ρ_j is the jam density. The KK equilibrium function is a monotonously decreasing function with respect to ρ, reaches the minimum 0 at the jam density, and possesses a turning point which is necessary for the derivation of the modified KdV equation [28, 29]. Moreover, stability criteria dependent on the equilibrium function need to contain the unstable condition because the traffic flow is unstable in one density or velocity subinterval.

The stability distribution of continuum traffic flow models along the whole density range abides by the following rule: stable at low density $\longrightarrow$ metastable $\longrightarrow$ unstable at medium density $\longrightarrow$ metastable $\longrightarrow$ stable at higher density, and in general the

dimensionless unstable density region is about $(0.15, 0.4)$ [8, 9, 23, 24]. According to this rule, we can determine the range of the pressure parameter by (26) with the KK equilibrium function:

$$p(\rho) = \rho^\gamma, \quad 0.1 < \gamma < 1.2. \tag{28}$$

Up to now, the propagation stability for (1) and (2) can thus be analyzed in terms of the initial condition $v_1(0)$ and the parameter α, and the pressure term has been determined by the stability criterion and the KK equilibrium function. We have programmed the completed ARA model with WENO schemes and succeeded in simulating the cluster and KdV soliton (the latter will be described in detail in section 4), which shows that the ARA model possesses the same numerical-simulation capability as other continuum models and the method of determining the pressure term is reasonable.

3. KdV equation. In order to obtain the unique weak solution of the nonlinear hyperbolic equation according to the weak solution theory and smoothing numerical solution, the continuum models always contain viscous terms, e.g., the KK model and the LLK model [8, 9, 10, 11]. Therefore it is necessary especially for the derivation of the KdV equation that the right-hand side of (2) be added by a higher-order viscous term, e.g., $\mu\partial_x^2 v$, $\mu > 0$, for a stable solution [9, 15, 30, 31]. We decompose the traffic flow into a linear combination of Fourier modes, each of which grows or decays with its own growth rate [30]. Thus we write

$$\rho(x,t) = \rho_0 + \sum_k \hat{\rho}_k \exp(ikx + \sigma_k t), \tag{29}$$

$$v(x,t) = v_0 + \sum_k \hat{v}_k \exp(ikx + \sigma_k t). \tag{30}$$

Substitute (29) and (30) into (1) and (2) with the viscous term, and linearize in $\hat{\rho}_k$ and $\hat{v}_k$. We find that each linear growth rate σ_k must satisfy the quadratic equation

$$0 = (ikv_0 + \sigma_k)^2 + \left(\frac{\mu}{\rho_0}k^2 - i\gamma\rho_0{}^\gamma k + \tau^{-1}\right)(ikv_0 + \sigma_k) + i\tau^{-1}V'\rho_0 k. \tag{31}$$

Both roots of (31) have negative real parts provided

$$V_\rho^0 + \gamma\rho_0^{\gamma-1} > 0, \tag{32}$$

while otherwise one root has a positive real part. (32) is an equivalent form of (26). (29)–(32) are the products of one kind of linear stability method, and the traffic flow is stable against all infinitesimal disturbances if they satisfy the linear stability condition (32). The neutral stability condition is

$$\eta \equiv V_\rho + \gamma\rho^{\gamma-1}|_{\rho=\rho_0} = 0. \tag{33}$$

The nonlinear stability analysis in section 2 is to take Taylor series expansions at the location of the wavefront, retain the constant and the first-order terms, obtain an ordinary differential equation, and finally determine the stability conditions by the convergence of solutions. However, the linear stability analysis in this section is to take Fourier series expansions with respect to the density and the velocity, linearize in the small density and velocity disturbances, obtain a quadratic equation of the growth rate

of Fourier modes, and ultimately determine the stability conditions only by judging the sign of the real parts of roots of the quadratic equation. The linear stability analysis cannot accurately distinguish each stability condition or present the stability evolution like Table 1. Moreover, there is another easier method to judge the stability according to the wave propagation rule: a higher-order partial differential equation with respect to small disturbances of the density and velocity can be obtained after the linearization of (1) and (2), the propagation speeds in the highest-order derivatives always determine the fastest and slowest signals, and the kinematic wave speed must intervene between the speeds of the fastest and slowest signals [1]. This is the so-called subcharacteristic condition, which is exactly another linear stability criterion [32]. Compared with the subcharacteristic conditions, the linear stability analysis listed in (29)–(33) also has its own advantage, i.e., some further results about the frequency and amplitude of the complex function can be worked out as follows [30].

Expanding (31) with ik near the neutral stability point yields

$$\sigma_k = -c(\rho_0)ik + \tau {\rho_0}^2 V_\rho^0 \eta k^2 + \mu\tau V_\rho^0 ik^3 - \mu\tau^2 V_\rho^0 \left(2\rho_0 V_\rho^0 + \gamma {\rho_0}^\gamma\right) k^4 + O(k^5), \tag{34}$$

where $c(\rho_0) = v_0 + \rho_0 V_\rho^0$ is the wave velocity, i.e., (6). Suppose the density of traffic flow near the neutral stability point is slightly perturbed. We quantify this supposition by writing

$$\eta = V'(\rho_0 + \delta\rho) + p'(\rho_0 + \delta\rho) = (V_{\rho\rho}^0 + p_{\rho\rho}^0)\delta\rho \equiv \theta\xi^2. \tag{35}$$

We consider the slowly varying behavior at long wavelengths near the neutral stability line. We wish to extract slow scales for space variable x and time variable t. The real part of (34) is $\tau {\rho_0}^2 V_\rho^0 \eta k^2$ and $-\mu\tau^2 V_\rho^0 \left(2\rho_0 V_\rho^0 + \gamma {\rho_0}^\gamma\right) k^4$. In order to balance the two terms, k scales as $k \propto \xi$, which leads to the scaling relation $x \propto \xi^{-1}$. The imaginary part of (34) is $-c(\rho_0)ik$ and $\mu\tau V_\rho^0 ik^3$. Since $-c(\rho_0)ik$ can be eliminated by a reference frame moving with the velocity $c(\rho_0)$, t scales as $t \propto \xi^{-3}$. Therefore we define the slow variables X and T [30, 27, 28, 29]:

$$X = \xi(x - ct) \qquad \text{and} \qquad T = \xi^3 t. \tag{36}$$

Finally we expect that an amplitude equation would balance the linear growth term of order $\xi^4 A$ with a stabilizing nonlinear term of order A^3; thus, we expect that the disturbance saturates at a size of order ξ^2. We implement the scalings by writing

$$\rho(x,t) = \rho_0 + \xi^2 \hat{\rho}(X,T), \tag{37}$$

$$v(x,t) = v_0 + \xi^2 \hat{v}(X,T). \tag{38}$$

Expanding each term in (1) and (2) added by $\mu\partial_x^2 v$ to the fifth order of ξ leads to the following nonlinear partial differential equations:

$$\xi^3 \left(-c\frac{\partial\hat{\rho}}{\partial X} + \rho_0 \frac{\partial\hat{v}}{\partial X} + v_0 \frac{\partial\hat{\rho}}{\partial X}\right) + \xi^5 \left(\frac{\partial\hat{\rho}}{\partial T} + \hat{\rho}\frac{\partial\hat{v}}{\partial X} + \hat{v}\frac{\partial\hat{\rho}}{\partial X}\right) = 0, \tag{39}$$

$$\begin{aligned} &\xi^2 \left(\rho_0\hat{v} - \rho_0 V_\rho^0 \hat{\rho}\right) + \xi^3 \left(-c\tau\rho_0 \frac{\partial\hat{v}}{\partial X} + V\tau\rho_0 \frac{\partial\hat{v}}{\partial X} - c\tau\gamma{\rho_0}^\gamma \frac{\partial\hat{\rho}}{\partial X} + V\tau\gamma{\rho_0}^\gamma \frac{\partial\hat{\rho}}{\partial X}\right) \\ &+\xi^4 \left(\hat{\rho}\hat{v} - V_\rho^0 \hat{\rho}^2 - \frac{1}{2}\rho_0 V_{\rho\rho}^0 \hat{\rho}^2 - \mu\tau\frac{\partial^2\hat{v}}{\partial X^2}\right) + \xi^5 \left(\tau\rho_0 \frac{\partial\hat{v}}{\partial T} + \tau\gamma{\rho_0}^\gamma \frac{\partial\hat{\rho}}{\partial X} + \tau\rho_0\hat{v}\frac{\partial\hat{v}}{\partial X}\right. \\ &\left. -\tau c\hat{\rho}\frac{\partial\hat{v}}{\partial X} + \tau V^0 \hat{\rho}\frac{\partial\hat{v}}{\partial X} + \tau\gamma{\rho_0}^\gamma \hat{v}\frac{\partial\hat{\rho}}{\partial X} - c\tau\gamma^2{\rho_0}^{\gamma-1}\hat{\rho}\frac{\partial\hat{\rho}}{\partial X} + V^0\tau\gamma^2{\rho_0}^{\gamma-1}\hat{\rho}\frac{\partial\hat{\rho}}{\partial X}\right) = 0. \end{aligned} \tag{40}$$

The third-order term of ξ can be rewritten as

(41)
$$\xi^3\left(-c\tau\rho_0\frac{\partial\hat{v}}{\partial X}+V\tau\rho_0\frac{\partial\hat{v}}{\partial X}-c\tau\gamma{\rho_0}^{\gamma}\frac{\partial\hat{\rho}}{\partial X}+V\tau\gamma{\rho_0}^{\gamma}\frac{\partial\hat{\rho}}{\partial X}\right)=-\xi^5\left(\theta\tau V_\rho^0\rho_0^2\frac{\partial\hat{\rho}}{\partial X}\right).$$

From the second-order term of ξ, we obtain

$$\hat{v}=V_\rho^0\hat{\rho}+O(\xi^2). \tag{42}$$

From the fourth-order and fifth-order terms of ξ, we obtain

$$\begin{aligned}\hat{q}\equiv\hat{\rho}\hat{v}=&\left(V_\rho^0+\frac{1}{2}\rho_0V_{\rho\rho}^0\right)\hat{\rho}^2+\mu\tau\frac{\partial^2\hat{v}}{\partial X^2}+\xi\tau\rho_0\left\{\tau\mu{V_\rho^0}^2\frac{\partial^3\hat{\rho}}{\partial X^3}+\left(\theta V_\rho^0\rho_0-\gamma{\rho_0}^{\gamma-1}\right)\frac{\partial\hat{\rho}}{\partial X}\right.\\&\left.+\left[2{V_\rho^0}^2+\rho_0V_\rho^0V_{\rho\rho}^0+(\gamma-\gamma^2)V_\rho^0{\rho_0}^{\gamma-1}\right]\hat{\rho}\frac{\partial\hat{\rho}}{\partial X}\right\}.\end{aligned} \tag{43}$$

Substituting (43) into the fifth-order term of ξ in (39) leads to the KdV equation with the perturbed term:

$$\begin{aligned}&\frac{\partial\hat{\rho}}{\partial T}+\left(2V_\rho^0+\rho_0V_{\rho\rho}^0\right)\hat{\rho}\frac{\partial\hat{\rho}}{\partial X}+\tau\mu V_\rho^0\frac{\partial^3\hat{\rho}}{\partial X^3}=-\xi\tau\rho_0\frac{\partial^2}{\partial X^2}\left\{\tau\mu{V_\rho^0}^2\frac{\partial^2\hat{\rho}}{\partial X^2}\right.\\&\left.+\left(\theta V_\rho^0\rho_0-\gamma{\rho_0}^{\gamma-1}\right)\hat{\rho}+\frac{1}{2}\left[2{V_\rho^0}^2+\rho_0V_\rho^0V_{\rho\rho}^0+(\gamma-\gamma^2)V_\rho^0{\rho_0}^{\gamma-1}\right]\hat{\rho}^2\right\}.\end{aligned} \tag{44}$$

In order to derive the regularized equation, we make the following transformations:

$$\hat{\rho}=\frac{-h}{2V_\rho^0+\rho_0V_{\rho\rho}^0}\hat{\rho}',\quad X=-\sqrt{\frac{-\tau\mu V_\rho^0}{h}}X',\quad\text{and}\quad T=\sqrt{\frac{-\tau\mu V_\rho^0}{h^3}}T', \tag{45}$$

where h is a constant. With the use of (45), one obtains the regularized equation:

$$\frac{\partial\hat{\rho}'}{\partial T'}+\hat{\rho}'\frac{\partial\hat{\rho}'}{\partial X'}+\frac{\partial^3\hat{\rho}'}{\partial X'^3}=-\xi A_1\frac{\partial^2}{\partial X'^2}\left[A_2\frac{\partial^2\hat{\rho}'}{\partial X'^2}+A_3\hat{\rho}'+A_4\hat{\rho}'^2\right], \tag{46}$$

where A_1, A_2, A_3, and A_4 are constant coefficients. If one ignores the $O(\varepsilon)$ terms in (46), it is just the KdV equation with a soliton solution as the desired solution:

$$\hat{\rho}'(X',T')=A\,\mathrm{sech}^2\left[\sqrt{\frac{A}{12}}\left(X'-\frac{A}{3}T'\right)\right]. \tag{47}$$

Amplitude A of soliton solutions of the KdV equation is a free parameter. The disturbance term $O(\xi)$ of the perturbed KdV equation (46) selects a unique member of the continuous family of KdV solitons.

Next, assuming that $\hat{\rho}'(X',T')=\hat{\rho}_0'(X',T')+\xi\hat{\rho}_1'(X',T')$, we take into account the $O(\xi)$ correction. In order to determine the selected value of A for the soliton solution (47), it is necessary to satisfy the solvability condition:

$$(\hat{\rho}_0',M[\hat{\rho}_0'])\equiv\int_{-\infty}^{\infty}\hat{\rho}_0'M[\hat{\rho}_0']dX'=0, \tag{48}$$

where $M[\hat{\rho}_0']$ is the $O(\xi)$ term of (46).

By performing the integration in the solvability condition (48), one obtains the selected value

$$A = -\frac{7\theta\rho_0\left(2V_\rho^0 + \rho_0 V_{\rho\rho}^0\right)}{4h(1-\gamma)V_\rho^0}. \tag{49}$$

Rewriting each variable to the original one leads to the soliton solution of the density:

(50)

$$\rho = \rho_0 + \frac{7\eta\rho_0}{4(1-\gamma)V_\rho^0}\operatorname{sech}^2\left\{\sqrt{\frac{7\eta\rho_0\left(2V_\rho^0+\rho_0V_{\rho\rho}^0\right)}{48\tau\mu(1-\gamma)V_\rho^{0^2}}}\left[x - ct + \frac{7\eta\rho_0\left(2V_\rho^0+\rho_0V_{\rho\rho}^0\right)}{12(1-\gamma)V_\rho^0}t\right]\right\}.$$

4. Numerical schemes. In this section, we will use the KdV soliton simulation to examine the analytical solution (50) and also to demonstrate that the ARA model can be used to reproduce the nonlinear traffic behaviors in real traffic. Because the solitary wave is a constant-shape traveling wave solution, we use WENO schemes to conduct numerical simulation. WENO schemes are high-order accurate finite difference schemes designed for the problems with piecewise smooth solutions containing discontinuities for hyperbolic conservation laws. The key idea lies at the approximation level, where a nonlinear adaptive procedure is used to automatically choose the locally smoothest stencil, hence avoiding crossing discontinuities in the interpolation procedure as much as possible. WENO schemes have been quite successful in applications, especially for problems containing both shocks and complicated smooth solution structures [33, 34, 35]. Because (3) with the viscous term is in the hyperbolic conservative form, λ_1 admits either shock waves or rarefactions, and $v_1(t)$ in (21) may be divergent, WENO schemes fit for the simulation of a unique smooth solution of nonlinear hyperbolic equations. Therefore, WENO schemes developed in [33, 34, 35] will be used in the following.

Let $\hat{f}$ be the numerical flux function corresponding to the flux f of (3) with the viscous term. Then, a standard conservative scheme of (3) with the viscous term reads as follows:

$$\frac{dY_i}{dt} + \frac{1}{\Delta x}(\hat{f}_{i+1/2} - \hat{f}_{i-1/2}) = g(Y_i). \tag{51}$$

In the following, the numerical flux $\hat{f}_{i+1/2}$ is reconstructed by the WENO method through the Lax–Friedrichs flux splitting. The third-order accurate WENO finite difference scheme applies the cell point values $\{Y_j\}_{j=i-1}^{i+1}$ to reconstruct $Y_{i+1/2}^-$, which is the cell boundary value of $x_{i+1/2}$ on the left-hand side. With $\{Y_j\}_{j=i}^{i+2}$, $Y_{i+1/2}^+$ is similarly constructed and is the cell boundary value of $x_{i+1/2}$ on the right-hand side. Thus, we use the Lax–Friedrichs numerical flux as follow:

$$\hat{f}_{i+1/2} = \frac{1}{2}\left[f\left(Y_{i+1/2}^-\right) + f\left(Y_{i+1/2}^+\right) - \alpha\left(Y_{i+1/2}^+ - Y_{i+1/2}^-\right)\right]. \tag{52}$$

(51) and (52) constitute a complete semidiscretized scheme. We apply the third-order accurate TVD Runge–Kutta time discretization, for which the semidiscrete scheme (51) is written as the ODEs: $Y_t = L(Y)$.

The equilibrium function in (1) and (2) with the viscous term is displaced by (27), and the dimensionless unstable region of the traffic system (3) with the viscous term, $(0.105, 0.414)$, can be obtained from (26) or (32). We design a density disturbance in

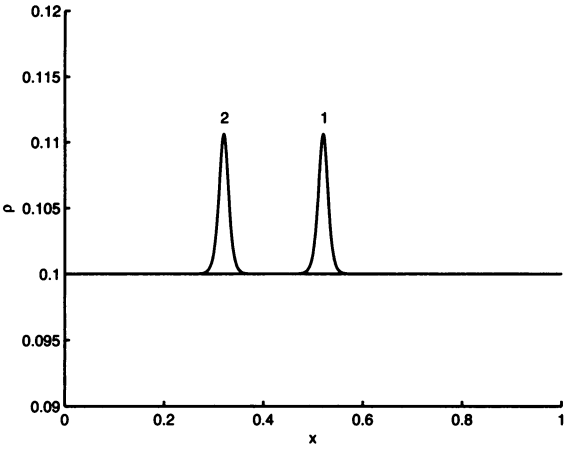

FIG. 4. *The analytical solution with* $\mu = 0.05$, (50).

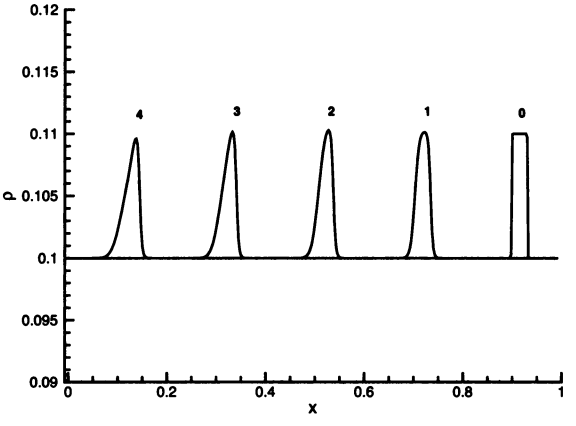

FIG. 5. *The numerical density solution in* 0, $0\triangle t$; 1, $3000\triangle t$; 2, $6000\triangle t$; 3, $9000\triangle t$; *and* 4, $12000\triangle t$.

the steady state as an initial condition:

$$\rho(x,0) = \begin{cases} \rho_0 + \hat{\rho} & x_0 - l \le x \le x_0 + l, \\ \rho_0 & \text{otherwise}, \end{cases} \tag{53}$$

where $\hat{\rho}$ is a small perturbation. The initial velocity is given by (27). The basic parameters are the pressure parameter $\gamma = 0.8$, the free velocity $v_f = 30$ m/s, the road length $L = 15000$ m, the relaxation time $\tau = 12$ s, the space interval $\triangle x = 37.5$ m, the perturbed radius $l = 0.03L$, and the dimensionless viscous coefficient $\mu = 0.05$ (see [10, 11]). The time interval $\triangle t$ must be less than 0.084 s for the numerical convergence, and we choose $\triangle t = 0.042$ s [11].

We have indeed obtained the numerical and analytical solutions of the KdV soliton near the neutral stability line as shown in Figures 4–6. In Figure 5, curve-1 is still affected by the initial condition (53) in $3000\triangle t$, and curve-2 in $6000\triangle t$ and curve-3 in $9000\triangle t$ are basically consistent with the analytic results in Figure 4. The amplitude, wave propagation velocity, and the basic shape of the numerical results are close to

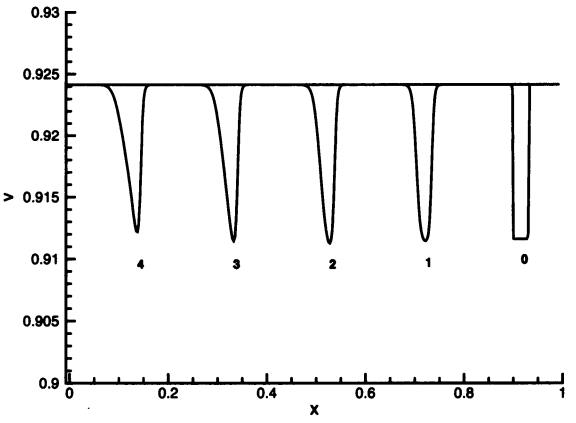

FIG. 6. *The numerical velocity solution in* 0, $0\triangle t$; 1, $3000\triangle t$; 2, $6000\triangle t$; 3, $9000\triangle t$;*and* 4, $12000\triangle t$.

those of the analytical solution, but the former are smoother than the latter, which may be caused by the numerical viscosity or the omission of the terms of the sixth and higher orders in the asymptotic expansion. Therefore the reduction perturbation method is superior to the semianalytical explanation in [31]. However, curve-4 in $12000\triangle t$ in Figure 5 shows that the dissipation term may decrease the amplitude, broaden the distribution, and contribute to an asymmetric effect. The propagation situation of the velocity is shown in Figure 6: the perturbed velocity profile is nearly symmetric to the perturbed density profile along the x-axis except the amplitude, which has examined our viewpoints in section 2. The consistency between the analytical and numerical results demonstrates that the reduction perturbation method in the continuum model originated by Kurtze and Hong [30] and further developed in this paper can really give the reasonable KdV soliton solution for traffic flow.

5. Summary. Considering that the previous two-equation models mimicked the gas dynamics equations with an unrealistic dependence on the acceleration with respect to the space derivative of the traffic pressure and consequently led to nonphysical effects, Aw and Rascle proposed the ARA model by replacing the space derivative with a convective derivative and rigidly discussed the solution to the Riemann problem and the admissibility of the elementary waves by the hyperbolic conservation laws. In this paper, we have discussed the application of the ARA model to investigating the traffic flow by the nonlinear stability and wave analyses. We have taken the nonlinear stability analysis on the ARA model through the wavefront expansion method. In comparison with the linear stability analysis, the nonlinear stability analysis additionally gives the analytical solution of the slope of the wavefront, and then the evolution of disturbances with time can be illuminated by stability parameters and initial conditions. We used the stability results to determine the anticipation factor. We obtained the KdV equation and analytical soliton solution from the "viscous" ARA model near the neutral stability line by extracting slow scales for space and time variables with the reduction perturbation method. The derivation of the KdV equation in the viscous continuum ARA model is similar to that in the car-following models but is more difficult because the continuum model has two equations. We applied WENO schemes to simulating the KdV soliton, and the simulation result is consistent with the analytical solution of the soliton density wave.

Acknowledgment. The authors are deeply appreciative to the referees for the insight represented in their constructive comments and suggestions.

REFERENCES

[1] G. B. WHITHAM, *Linear and Nonlinear Waves*, John Wiley and Sons, Inc., New York, 1974.
[2] P. I. RICHARDS, *Shockwaves on the highway*, Oper. Res., 4 (1956), pp. 42–51.
[3] M. J. LIGHTHILL AND G. B. WHITMAN, *On kinematic waves:* II. *A theory of traffic flows on long crowded roads*, in Proceedings of the Royal Society, Series A, 229 (1955), pp. 317–345.
[4] H. J. PAYNE, *Models of freeway traffic and control*, in Mathematical Models of Public Systems Simulation Council Proc. Ser. 28, Vol. 1, Simulation Council, New York, 1971, pp. 51–61.
[5] H. J. PAYNE, *FREFLO: A macroscopic simulation model of freeway traffic*, Transport. Res. Record, 772 (1979), pp. 68–75.
[6] R. D. KÜHNE, *Macroscopic freeway model for dense traffic—Stop-start waves and incident detection*, in Proceedings of the 9th International Symposium on Transportation and Traffic Theory, I. Volmuller and R. Hamerslag, eds., VNU Science Press, Utecht, The Netherlands, 1984, pp. 21–42.
[7] R. D. KÜHNE, *Freeway speed distribution and acceleration noise—Calculations from a stochastic continuum theory and comparison with measurements*, in Proceedings of the 10th International Symposium on Transportation and Traffic Theory, N. H. Garter and N. H. M. Wilson, eds., Elsevier, New York, 1987, pp. 119–137.
[8] B. S. KERNER AND P. KONHÄUSER, *Cluster effect in initially homogeneous traffic flow*, Phys. Rev. E, 48 (1993), pp. R2335–R2338.
[9] B. S. KERNER AND P. KONHÄUSER, *Structure and parameters of clusters in traffic flow*, Phys. Rev. E, 50 (1994), pp. 54–83.
[10] H. Y. LEE, H. W. LEE, AND D. KIM, *Origin of synchronized traffic flow on highways and its dynamic phase transitions*, Phys. Rev. Lett., 81 (1998), pp. 1130–1133.
[11] H. Y. LEE, H. W. LEE, AND D. KIM, *Dynamic states of a continuum traffic equation with on-ramp*, Phys. Rev. E, 59 (1999), pp. 5101–5111.
[12] D. HELBING, *Gas-kinetic derivation of Navier-Stokes-like traffic equation*, Phys. Rev. E, 53 (1996), pp. 2366–2381.
[13] D. HELBING, *Derivation and emprical validation of a refined traffic flow model*, Phys. A, 233 (1996), pp. 253–282.
[14] M. TREIBER, A. HENNECKE, AND D. HELBING, *Derivation, properties, and simulation of a gas-kinetic-based, non-local traffic model*, Phys. Rev. E, 59 (1999), pp. 239–253.
[15] D. HELBING, *Micro- and macro-simulation of freeway traffic*, Math. Comput. Modelling, 35 (2002), pp. 517–547.
[16] C. DAGANZO, *Requiem for second-order fluid approximation to traffic flow*, Trans. Res. B, 29 (1995), pp. 277–286.
[17] A. AW AND M. RASCLE, *Resurrection of "second order" models of traffic flow*, SIAM J. Appl. Math., 60 (2000), pp. 916–938.
[18] M. RASCLE, *An improved macroscopic model of traffic flow: Derivation and links with the Lighthill-Whitham model*, Math. Comput. Modelling, 35 (2002), pp. 581–590.
[19] A. KLAR AND R. WEGENER, *Kinetic derivation of macroscopic anticipation models for vehicular traffic*, SIAM J. Appl. Math., 60 (2000), pp. 1749–1766.
[20] R. JIANG, Q. S. WU, AND Z. J. ZHU, *A new continuum model for traffic flow and numerical tests*, Transport. Res. B, 36 (2002), pp. 405–419.
[21] Y. XUE AND S. Q. DAI, *Continuum traffic model with the consideration of two delay time scales*, Phys. Rev. E, 68 (2003), pp. 066123.
[22] J. G. YI, H. LIN, L. ALVAREZ, AND R. HOROWITZ, *Stability of macroscopic traffic flow modeling through wavefront exapansion*, Transport. Res. B, 37 (2003), pp. 661–679.
[23] Z. H. OU, *Equlibrium functions of traffic flow*, Phys. A, 351 (2005), pp. 620–636.
[24] Z. H. OU, S. Q. DAI, L. Y. DONG, Z. WU, AND M. D. TAO, *New equilibrium function of traffic flow*, Phys. A, 362 (2006), pp. 525–531.
[25] H. M. ZHANG, *Analyses of the stability and wave properties of a new continuum traffic theory*, Transport. Res. B, 33 (1999), pp. 299–415.
[26] H. M. ZHANG, *A non-equilibrium traffic model devoid of gas-like behavior*, Transport. Res. B, 36 (2002), pp. 275–290.
[27] T. KOMATSU AND S. SASA, *Kink soliton characterizing traffic congestion*, Phys. Rev. E, 52 (1995), pp. 5574–5582.
[28] M. MURAMATSU AND T. NAGATANI, *Soliton and kink jams in traffic flow with open boundaries*, Phys. Rev. E, 60 (1999), pp. 180–187.

[29] Z. H. Ou, S. Q. Dai, and L. Y. Dong, *Density waves in the full velocity difference model*, J. Phys. A, 39 (2006), pp. 1251–1263.
[30] D. A. Kurtze and D. C. Hong, *Traffic jams, granular flow, and soliton selection*, Phys. Rev. E, 52 (1995), pp. 218–221.
[31] P. Berg and A. W. Woods, *On-ramp simulations and solitary waves of a car-following model*, Phys. Rev. E, 64 (2001), pp. 035602.
[32] A. Aw, A. Klar, T. Materne, and M. Rascle, *Derivation of continuum traffic flow models from microscopic follow-the-leader models*, SIAM J. Appl. Math., 63 (2000), pp. 259–278.
[33] A. Harten, B. Engquish, S. Osher, and S. Chakravarthy, *Uniformly high order essentially non-oscillatory schemes*, III, J. Comput. Phys., 71 (1987), pp. 231–303.
[34] C.-W. Shu, *Essentially non-oscillatory and weighted essentially non-oscillatory schemes for hyperbolic conservation laws*, in Advanced Numerical Approximation of Numerical Hyperbolic Equations, B. Cockburn, C. Johnson, C.-W. Shu, and E. Tadmor, eds., Lecture Notes in Math. 1697, A. Quarteroni, ed., Springer, New York, 1998, pp. 325–432.
[35] P. Zhang, S. C. Wong, and C.-W. Shu, *A weighted essentially non-oscillatory numerical scheme for a multi-class traffic flow model on an inhomogeneous highway*, J. Comput. Phys., 212 (2006), pp. 739–756.